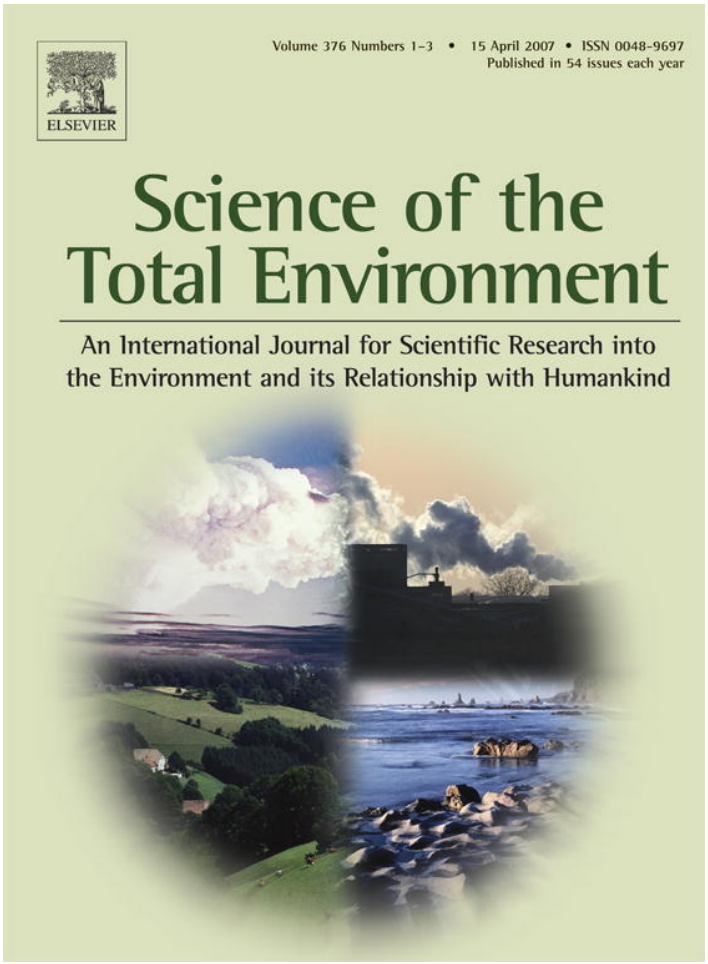

Available online at www.sciencedirect.com
ScienceDirect
Science of the Total Environment 376 (2007) 294–305
Science of the Total Environment
An International Journal for Scientific Research into the Environment and its Relationship with Humankind
www.elsevier.com/locate/scitotenv

Characterization of U/Pu particles originating from the nuclear weapon accidents at Palomares, Spain, 1966 and Thule, Greenland, 1968

O.C. Lind [a,*], B. Salbu [a], K. Janssens [b], K. Proost [b], M. García-León [c], R. García-Tenorio [c]

[a] *Isotope Laboratory, Norwegian University of Life Sciences, P.O. Box 5003, 1432 Ås, Norway*
[b] *Department of Chemistry, University of Antwerp, Universiteitsplein 1, B-2610 Antwerp, Belgium*
[c] *Applied Nuclear Physics Group, University of Seville, Avda. Reina Mercedes, 41012-Seville, Spain*

Received 6 July 2006; received in revised form 16 November 2006; accepted 22 November 2006
Available online 2 March 2007

Abstract

Following the USAF B-52 bomber accidents at Palomares, Spain in 1966 and at Thule, Greenland in 1968, radioactive particles containing uranium (U) and plutonium (Pu) were dispersed into the environment. To improve long-term environmental impact assessments for the contaminated ecosystems, particles from the two sites have been isolated and characterized with respect to properties influencing particle weathering rates. Low $^{239}Pu/^{235}U$ (0.62–0.78) and $^{240}Pu/^{239}Pu$ (0.055–0.061) atom ratios in individual particles from both sites obtained by Inductively Coupled Plasma Mass Spectrometry (ICP-MS) show that the particles contain highly enriched U and weapon-grade Pu. Furthermore, results from electron microscopy with Energy Dispersive X-ray analysis (EDX) and synchrotron radiation (SR) based micrometer-scale X-ray fluorescence (μ-XRF) 2D mapping demonstrated that U and Pu coexist throughout the 1–50 μm sized particles, while surface heterogeneities were observed in EDX line scans. SR-based micrometer-scale X-ray Absorption Near Edge Structure Spectroscopy (μ-XANES) showed that the particles consisted of an oxide mixture of U (predominately UO_2 with the presence of U_3O_8) and Pu ((III)/(IV), (IV)/(V) or (III), (IV) and (V)). Neither metallic U or Pu nor uranyl or Pu(VI) could be observed. Characteristics such as elemental distributions, morphology and oxidation states are remarkably similar for the Palomares and Thule particles, reflecting that they originate from similar source and release scenarios. Thus, these particle characteristics are more dependent on the original material from which the particles are derived (source) and the formation of particles (release scenario) than the environmental conditions to which the particles have been exposed since the late 1960s.

Keywords: U/Pu particles; Electron microscopy; Synchrotron radiation; Micro-XRF; Micro-XANES; Element and isotope ratios

1. Introduction

On the morning of the 17th of January 1966, a US Air Force B-52 bomber carrying four 1.5 Mt thermonuclear bombs collided with a KC-135 fuel tanker aircraft during a refuelling operation over Southern Spain. Both aircrafts caught fire at an altitude of 8500 m above the village of Palomares and subsequently exploded (Iranzo et al., 1987). The nuclear weapons were released from the B-52 bomber and two of the bombs detonated conventionally upon impact on land. The explosion and subsequent fire

* Corresponding author. Tel.: +47 64 96 5545; fax: +47 64 94 8359.
E-mail address: olelin@umb.no (O.C. Lind).

0048-9697/$ - see front matter © 2006 Elsevier B.V. All rights reserved.
doi:10.1016/j.scitotenv.2006.11.050

(nuclear fuel partially burned) caused the dispersion of particles containing Pu and U (Lind et al., 2004; Jiménez-Ramos et al., 2006) over a terrestrial area of about 2.3 km^2 (Iranzo et al., 1987) situated close to the Mediterranean. A similar accident occurred at Thule, Greenland, 1968, where a B-52 bomber carrying four thermonuclear bombs caught fire and crashed on the ice at Bylot Sound. Due to explosive fire, particles containing Pu and U (Eriksson, 2002; Lind et al., 2005) were dispersed over the ice within a distance of a few kilometres and some of the fissile material has been located within the sediments of Bylot Sound (Aarkrog, 1971).

To assess the environmental impact of radioactive particles released from weapon-grade material and deposited in ecosystems, detailed information is required on particle characteristics such as size, composition, morphological structure and oxidation states of matrix elements such as U and Pu, influencing particle weathering rates and subsequent mobilization of radionuclides from particles present in soil–water and sediment–water systems (Salbu, 2000b). Previous studies of radioactive particles released from different nuclear sources under different release conditions, such as reactor accidents involving explosions or fires, have demonstrated that the particle characteristics are source and release scenario dependent (Salbu, 2000a). A key property influencing the radioecological behaviour of U and Pu is their oxidation state (Silva and Nitsche, 2001; Choppin, 2003). Uranium chemistry predicts that particle weathering rate (y^{-1}) increases with the oxidation state for U and should be higher for U_3O_8 particles than for UO_2 (Kashparov et al., 1999). Although experimental solubility data reported for Pu oxides/hydroxides scatter widely (Runde et al., 2002), the solubility products of $Pu(OH)_3$ [$K°sp = 10^{-26.2\pm0.8}$, (Felmy et al., 1989)], tetravalent Pu [$Pu(OH)_4$, $K°sp = 10^{-58.7\pm0.9}$ (Knopp et al., 1999); PuO_2, $K°sp = 10^{-63.8\pm1}$ (Kim and Kanellakopulos, 1989)] and pentavalent PuO_2OH [$K°sp = 10^{-9.3}$, (Zaitseva et al., 1968)], indicate that particle weathering rates will strongly depend on the oxidation state of Pu. Although information on a limited number of particles cannot be considered to be representative for the whole contaminated area, the information on solid-state speciation including oxidation states will be essential in environmental impact assessments. Once U and Pu are in a solution, their overall mobility is governed by the environmental conditions (e.g., soil–water pH and concentration of interacting agents, redox conditions and microbial activity).

From the fact that these particles have persisted in the environment for decades it is obvious that the weathering rates have been rather slow. On the other hand, recent reports (García-Tenorio et al., 2004; Espinosa et al., 2005) suggest that Pu in Palomares soils is becoming more mobilised and potentially bioavailable as a result of natural weathering and agricultural practices (e.g. irrigation and fertilization). Pu extracted from contaminated Palomares soils (4 g) by distilled H_2O in 24 h increased by two orders of magnitude from 1986 to 2001 and up to 14% of Pu in soil (4 g) was extracted by cow urine in 24 h (Espinosa et al., 2005). To understand and estimate the impact of such particle transformation processes, information on the solid-state speciation of the particle matrix elements is needed. The Palomares and Thule accidents provide a unique possibility to study long-term actinide behaviour in the environment including radioactive particle weathering. The source terms and release scenarios are similar, whereas the affected ecosystems and environmental compartments (i.e. temperate, semi-arid terrestrial vs. arctic, marine benthic) in which the particles have resided are very different.

In the present work, individual radioactive particles extracted from contaminated soil and sediment samples collected at Palomares and Thule (Lind et al., 2005) have been characterized with respect to size, 2D elemental composition and distribution, morphology and oxidation states as well as isotopic composition. Non-destructive analyses were performed using γ-spectrometry, scanning electron microscopy (SEM) and Environmental Scanning Electron Microscope (ESEM) in combination with Energy Dispersive X-ray analysis (SEM–EDX and ESEM–EDX) as well as synchrotron radiation (SR) based microscopic techniques. The SR-based microscopic techniques were especially developed for characterization of particles containing U (Salbu et al., 2003; Lind et al., 2005). SR-based micro-X-ray fluorescence (μ-SRXRF) provides information on the elemental composition of the particles, while SR-based micro-X-ray absorption near edge structure (μ-XANES) spectroscopy provides information on oxidation states of U and Pu. Finally, ICP-MS analyses of dissolved individual particles reveal the isotopic composition of the actinides. Although the number of analysed particles is limited, the study on individual particles should provide detailed information on the phenomenon of accidentally released radioactive particles in the environment *per se*.

2. Materials and methods

2.1. Sampling and isolation of particles

2.1.1. Palomares

Two 10 cm soil cores were collected in 2001 from a contaminated area, located to the west of the Palomares village (Fig. 1). Each sample was air dried and divided

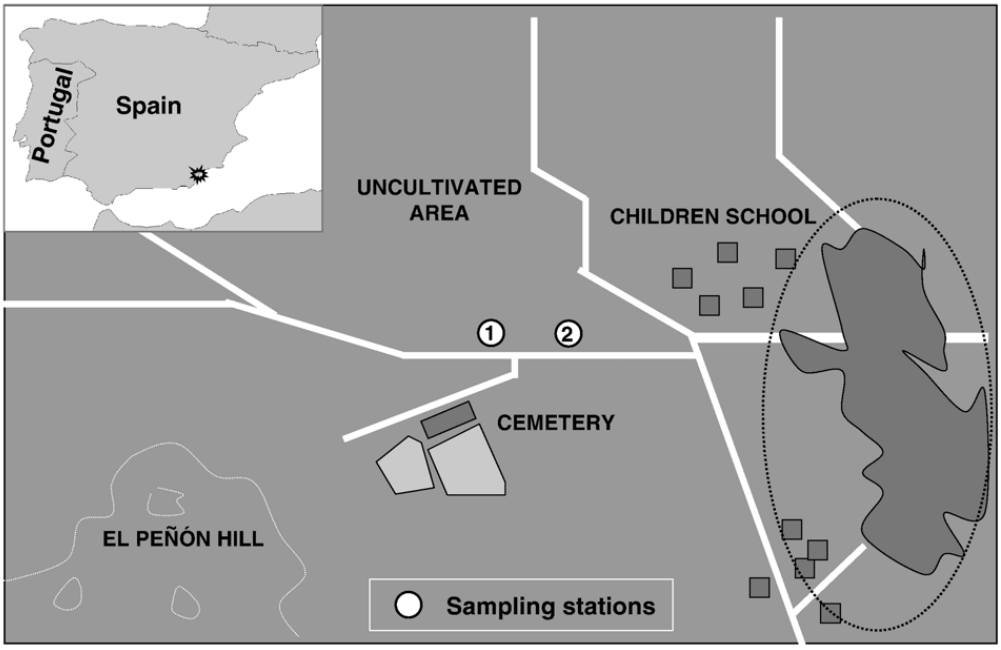

Fig. 1. The sampling sites located outside the village of Palomares (highlighted), province of Almería, Spain. The explosive fire of one of the nuclear weapons affected the zone to the West of the village.

into 6 aliquots to be measured by gamma spectrometry. Elevated activity concentrations of ^{241}Am (E_γ = 59.5 keV) indicating the presence of ^{241}Pu were found in one aliquot from each of the two cores. From these aliquots a few soil grains were isolated from the matrix by performing successive divisions and measuring the subsamples by means of γ-spectrometry. The isolated soil grains were fixed onto carbon double-faced sticky tape and mounted onto Al stubs for further identification of particles in Scanning Electron Microscopy with Energy Dispersive X-ray analysis (SEM–EDX, Section 2.2). Based on information from SEM–EDX images and γ-spectrometry, 8 particles were identified and 5 single particles were fully isolated from the residual. The individual radioactive particles were counted 6 mm above the surface of a Low Energy Germanium (LEGe) detector (Canberra, rel. efficiency 25%, resolution 1.8 keV) using a purpose-built geometry setup.

2.1.2. Thule

Sampling was performed onboard the Greenland fisheries research vessel "Adolf Jensen" during the August 1997 expedition in Bylot Sound (Dahlgaard et al., 2001). Thule sediments were sampled just below the point of impact using a Gemini corer and subsequently kept frozen. Aliquots of the ~5 kg sediment sample were carefully melted (room temperature), air dried and homogenized prior to isolation of individual particles, using γ-measurements and SEM–EDX as described. A set of 3 individual particles was identified and isolated as part of previously reported work (Lind et al., 2005).

After air drying, both Thule and Palomares bulk samples and isolated particles were kept in plastic boxes under ambient conditions (room temperature, normal atmosphere).

2.2. SEM and ESEM with EDX

Particles were further localised and characterized using a Jeol 840 Scanning Electron Microscope (SEM) for acquisition of digital images in both Secondary (SEI) and Backscattered (BEI) electron imaging modes. Energy Dispersive X-ray analysis, X-ray mapping (spatial resolution about 1 μm) and X-ray spot analysis were performed using a Link ISIS 300 X-ray analytical system (Oxford Instruments, Oxford, UK) including a Si (Li) detector attached to the SEM (Salbu et al., 2003). A Zeiss EVO 50 variable pressure Environmental Scanning Electron Microscope (ESEM) with an Inca EDX analytical system (Oxford Instruments, Oxford, UK) including a Si(Li) detector was utilized at high vacuum conditions to perform line scan analyses (spatial resolution about 1 μm) and acquisition of SEI and BEI-mode images of both Palomares and Thule particles. Peak intensities of U-Lα and Pu-Lα (12000–70000 counts per line scan) as well as Si $K\alpha_1$, Fe $K\alpha_1$ and Al $K\alpha_1$, X-ray lines were recorded at

15–18 nm increments along 6–20 μm lines from selected areas of the particle surfaces. In both instruments the acceleration voltage applied was 30 kV and collection of EDX data were performed with dead times of about 30%.

2.3. SR-based micro beam techniques

Individual particles characterized by SEM with EDX were subjected to SR-based μ-XRF and μ-XANES analysis using the same setup (focused 20×20 μm beam by using a polycapillary lens; HPGe detector) at the X-ray microscopic facility of beamline L, HASYLAB, Hamburg (Salbu et al., 2004). In order to determine the elemental distribution within individual particles, two dimensional μ-SRXRF mapping was performed by rastering (3 μm increments) the 20×20 μm beam over 70×70 μm^2 of the sample in the x–y plane with a 21 keV beam, which in these materials has a penetration depth of about 50 μm. Using μ-XANES, information on the oxidation state of U and Pu particles was obtained by tuning the monochromatic X-ray beam over the U L_{III} (17.163 keV) and Pu-L_{III} (18.057 keV) absorption edges while collecting X-ray fluorescence spectra at 1 eV increments from about 80 eV below to 220 eV above the U L_{III}-edge and from 60 eV below to 130 eV above the Pu-L_{III} -edge. The μ-XANES profile shapes and energy shifts of inflection points and white lines (i.e. the first strong resonance) of U in particles were compared with those of well-defined U oxidation state standards. For Pu no suitable reference compounds were available during the experiments. Thus, the procedure adopted in a previous study (Lind et al., 2005) was employed: the recorded μ-XANES Pu profiles were calibrated against XANES profiles obtained from Y and Zr reference foils and positioned on the same energy scale as profiles previously obtained for Pu(IV) (Panak et al., 2002) and Pu(III) (Conradson et al., 1998). The Pu(IV) XANES reference profile was recorded at the 41 beamline at the Stanford Synchrotron Radiation Laboratory using a Si (220) pair in the double crystal monochromator (1998). The Pu(III) XANES reference profile was digitized from Conradson et al. (1998) and recalibrated to the Zr–K edge energy at 17.998 keV. It is also assumed that the white line (WL) centroid energies of Pu(IV) in particles will fall within a narrow range of 18,067.9–18,068.7 eV as reported for several Pu(IV) compounds and solutions (Conradson et al., 2004a; Denecke, 2006).

The Pu-XANES profiles of the particles were qualitatively compared to published Pu-XANES profiles of solid compounds and standard solutions (Conradson et al., 1998, 2004a, 2005; Panak et al., 2002; Powell et al., 2006). Specifically, the position of the WL and inflection point as well as the energy difference between the WL centroid and that of the first scattering maximum past the WL (FSM) were used to differentiate between the oxidation states of Pu. The XANES edge energies were estimated based on the half-height of the edge step as described by Duff et al. (1999).

The following XANES spectra characteristics were applied for the differentiation of Pu oxidation states:

- Metallic Pu: the XANES profiles are typically characterized by a substantially diminished WL. The inflection point energy shift is approximately 2–3 eV lower than Pu(III) and about 5 eV lower than Pu(IV), while the WL centroid is only 1.3 eV lower than for PuO_2 (Conradson et al., 2004a).
- Pu(III): the WL centroid energies for solid compounds and solutions of Pu(III) are generally ≥2 eV lower than for Pu(IV) (Conradson et al., 2004a; Denecke, 2006). The energy difference between the WL centroid and FSM is ~30–33 eV for solutions (Conradson et al., 1998; Denecke, 2006).
- Pu(IV): the WL centroid energy of ordered PuO_2 is 18,068.6±0.3 eV, according to Conradson et al (2004a). The energy difference between the WL centroid and FSM is ~40 eV for PuO_2 (Powell et al., 2006).
- Pu(V): XANES energy positions (WL and inflection point) of Pu(V) are typically found midway between those of Pu(III) and Pu(IV) (Conradson et al., 2004a, 2005).
- Pu(VI): for solids, the XANES energies of Pu(VI) are ~7–8 eV (WL centroid) and ~3–4 eV (inflection point) higher than for Pu(IV) as estimated from published Pu-XANES profiles (Duff et al., 1999).

No significant changes of the XANES profiles were observed between replicate measurements of standards and samples indicating that artefacts due to radiation damage in the samples or standards did not take place. Our μ-XANES profiles were collected from both the cores and the outer spheres of the particles in an attempt to reveal possible inhomogeneities.

2.4. ICP-MS measurements

Following the characterization of particles by non-destructive techniques, one "typical" individual particle from each of the sites was sacrificed in order to determine the $^{240}Pu/^{239}Pu$ and $^{235}U/^{239}Pu$ atom ratios for source identification and characterization. The particles were partially dissolved by microwave boiling (72 Bar,

~280 °C) in suprapur HNO_3 (65%). The final solutions were filtered by Whatman GF/C filters. The yield (Palomares 29.0±1.1%; Thule 28.0±1.0%) of the microwave digestion was determined from ^{241}Am γ-measurements of the particle prior to the digestion and subsequently of the obtained filtered solution. The ^{240}Pu /^{239}Pu and ^{235}U/^{239}Pu atom ratios were determined by ICP-MS (Perkin-Elmer ELAN 6100) after radiochemical separations based on selective sorption on anion exchange resins (Dowex AG 1×8) to separate U and Am from Pu (Clacher, 1995). ^{242}Pu and ^{233}U were used as yield monitors.

3. Results and discussion

3.1. γ-spectrometry and ICP-MS

Based on γ-measurements of individual particles the ^{241}Am activities ranged from 0.2–13.5 Bq/particle for Palomares (n=5) and 1.0–2.7 Bq/particle for Thule (n=3) particles (Table 1). ICP-MS data showed the $^{239+240}$Pu activity and ^{240}Pu/^{239}Pu atom ratio of particle PB to be 42.6±5.9 Bq (1 SD) and 0.061±0.006, respectively. This atom ratio is in agreement with Chamizo et al. (2006), using Accelerator Mass Spectrometry to determine a mean ^{240}Pu/^{239}Pu atom ratio of 0.0657±0.0006 in soils containing elevated Pu activity concentrations (expressed in Bq/kg) from sampling station 2 (Fig. 1). For the Thule particle (TC), the corresponding ratio measured in our laboratory were 0.055±0.007 (Lind et al., 2005), somewhat lower than for the Palomares particle. According to Eriksson (2002), about two thirds of the Thule debris originated from a source having a ^{240}Pu/^{239}Pu isotope ratio of 0.056, whereas about one third of the debris featured a lower ^{240}Pu/^{239}Pu isotope ratio (0.027). Thus, the analysed Thule particle belongs to the high ^{240}Pu/^{239}Pu isotope ratio group.

By combining the γ-measurement data with the ICP-MS data, a ^{241}Am/$^{239+240}$Pu activity ratio of 0.19±0.02 could be calculated for the Palomares particle. That compares well with Irlweck and Hrnecek (1999), who found an ^{241}Am/$^{239+240}$Pu activity ratio of ~0.2 (corrected for in-growth of ^{241}Am from ^{241}Pu using ^{241}Pu/^{239}Pu data from Mitchell et al. (1997)) for a particle contaminated Palomares soil aliquot. The corresponding ratio obtained for the Thule particle analysed by us was 0.14±0.02 (Lind et al., 2005), which is somewhat lower than for the Palomares particle, and also lower than that reported for 5 Thule particles (average of five Thule particles ~0.19 (Eriksson, 2002), corrected for in-growth of ^{241}Am from ^{241}Pu using data from Mitchell et al. (1997)). However, our Thule result fall within the ^{241}Am/$^{239+240}$Pu activity ratio range of measured bulk Thule sediments (Dahlgaard et al., 2004).

Recent quadruple ICP-MS analysis showed that U in a totally digested hot particle isolated from highly contaminated Palomares soil was enriched with respect to ^{235}U. The measured ^{235}U/^{238}U atom ratio of 0.185 was about 25 times higher than in natural U, but the ratio may have been slightly biased due to a possible contamination of ^{238}U (Jiménez-Ramos et al., 2007). The Thule particles (n=5) were apparently more enriched with respect to ^{235}U than the Palomares particle, with an average ^{235}U/^{238}U atom ratio of 1.03±0.16 (Eriksson, 2002). The ICP-MS measurements of the particles in the present work yielded low ^{239}Pu/^{235}U atom ratios: 0.78±0.14 for the Palomares particle PB and 0.62±0.13 for the Thule particle TC, showing that ^{235}U constitutes the major part of the fissile material in both particles. The Thule particle results are supported by results of Eriksson (2002), who observed ^{239}Pu/^{235}U atom ratios for Thule particles ranging from 0.26–0.88.

We conclude from the above considerations that both Palomares and Thule particles contain a mixture of weapon-grade Pu and enriched U. Available information confirms that both materials are commonly used in nuclear warheads and can even be used in composite highly enriched U/weapon-grade Pu pits (Bukharin, 1998). The release of particles containing enriched U and Pu has also been observed following a nuclear warhead-carrying missile fire at the former US McGuire air force base (Drell and Peurifoy, 1994) as well as following the destruction of a nuclear warhead-carrying missile on the Johnston Atoll (Wolf et al., 1997).

Table 1
Sample information

Sampling station	Particle no.	Approx. particle size μm	^{241}Am Bq/particle (±SD)
Palomares			
1	PA	45	6.2±0.2
2	PB	35	8.0±0.1
Idem	PC	50	13.5±0.3
Idem	PD	40	12.3±0.4
Idem	PE	4	0.20±0.02
Idem	PF	3	n.m.
Idem	PG	4	n.m.
Idem	PH	1	n.m.
Thule			
Below point of impact	TA	35	1.6±0.1
Idem	TB	40	1.2±0.1
Idem	TC	20	2.8±0.05

Sampling stations, approximate sizes and ^{241}Am activities of particles. n.m.=not measured as individual particles were not fully isolated.

3.2. SEM/ESEM with EDX and μ-SRXRF

Using SEM in SEI and BEI-mode (Figs. 2 and 3), the size of the particles is estimated to be between 1 μm and 50 μm for Palomares and 20–40 μm for Thule (Table 1). However, the number of particles is limited and the ^{241}Am activity of submicron particles are below the detection limits (~0.1 Bq) for γ-spectrometry. In addition, the particles tend to be imbedded in larger soil and sediment aggregates and imbedded small sized particles are difficult to identify in SEM–EDX. Thus, the particle sizes reported herein should reflect the high end of the size distribution pattern.

In the electron microscopes, the particles appear as agglomerated crystalline grains with a relatively high degree of porosity (Figs. 2 and 3), indicating that the specific surface area of the particles may be relatively large. Solubility and particle weathering rates are expected to increase with increasing surface area available for weathering. All particles were partly covered with soil or sediment, which appears grey in the BEI images (i.e. low *Z* material). The soil in the Palomares area is of silica–carbonaceous nature (Jiménez-Ramos et al., 2006), which is reflected by the appearance of Al, Si and Fe in the EDX spectra.

Based on SEM–EDX (Fig. 2) and 2D μ-SRXRF (not shown) mapping, all investigated particles appear as a quite homogeneous mixture of U and Pu. While SEM–EDX mapping provide surface and to a certain extent subsurface information on elemental distribution, μ-SRXRF mapping is used to investigate depth-averaged compositional variation throughout the particles. Based

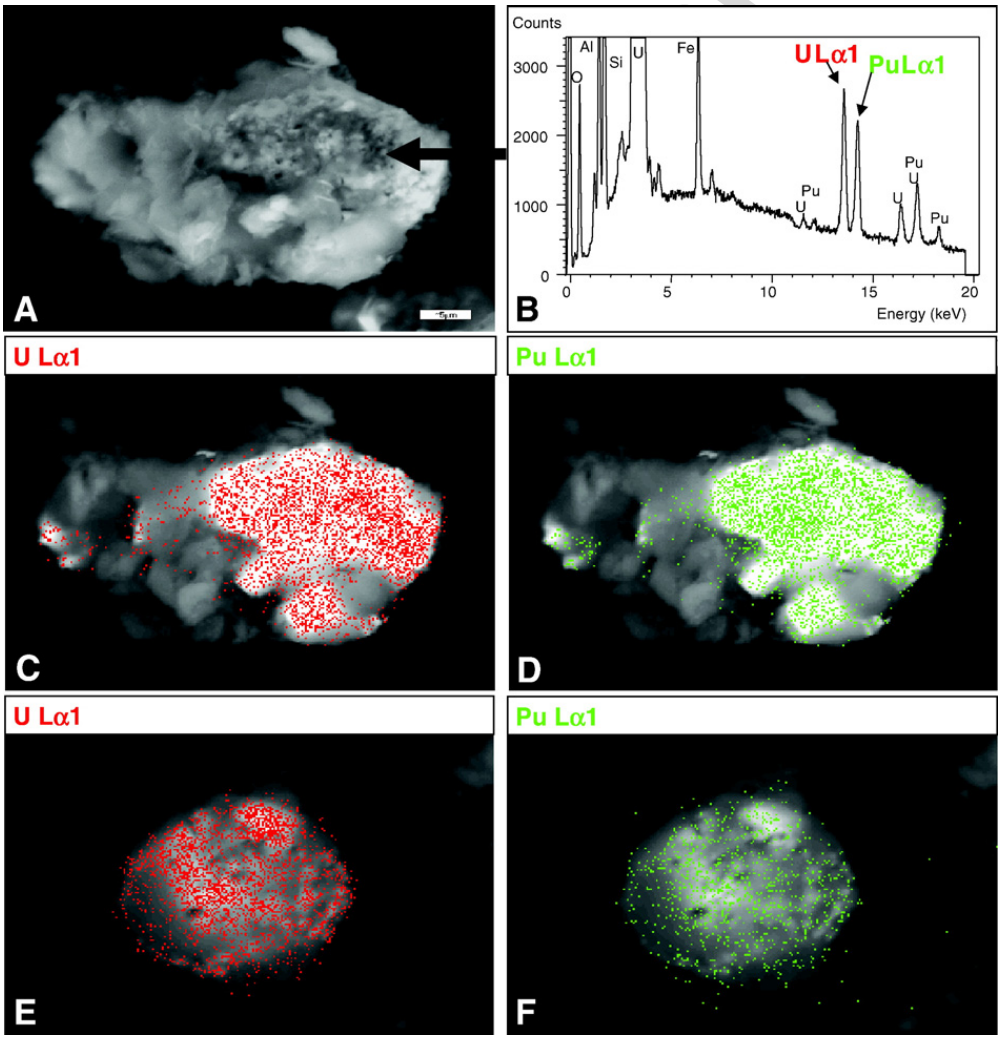

Fig. 2. Scanning electron microscopy (SEM) and Energy Dispersive X-ray analysis of particles PA isolated from Palomares soils (A–D) and TA (Lind et al., 2005) collected from Thule sediments (E–F). (A) SEM used in Secondary Electron Imaging (SEI) mode showing particle morphology. (B) EDX spectrum showing the elemental composition of the particle (analysis spot marked with arrow), (C) X-ray mapping of U superimposed on an image recorded in Backscattered Electron Imaging (BEI) mode image, (D) X-ray mapping of Pu superimposed on an image recorded in BEI. Bar 5 μm.

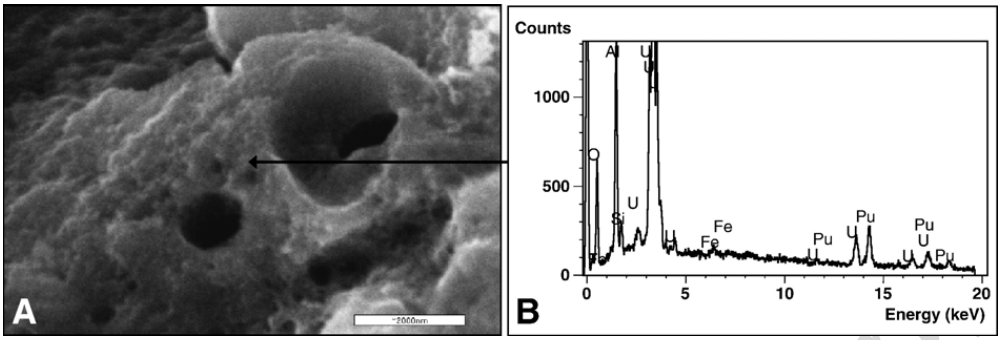

Fig. 3. SEM and EDX analysis of particle PC isolated from soils at Palomares, Spain. (A) SEM used in Secondary Electron Imaging (SEI) mode showing particle morphology. Note cavities and porosity of the material. Bar 2 μm. (B) EDX spectrum obtained from a spot in A (arrow). Al, Si and Fe, presumably from a coating of soil minerals, were detected in addition to U and Pu. Bar 2 μm.

on the observed U-Lα and Pu-Lα intensities in all pixels of scans obtained with the 20×20 μm beam, linear Pearson correlation coefficients of $r=0.997$ (PC) and $r=0.999$ (PD) were calculated for Palomares particles with a similarly high correlation ($r=0.999$) obtained for the Thule particle TA (Lind et al., 2005). Thus, at 20 μm scale U and Pu coexist throughout the particles, either as a consequence of the production of the fissile material or due to the explosion and subsequent fire. Based on Analytical Transmission Electron Microscopy (ATEM) and SEM–EDX, U and Pu coexisted also in radioactive particles released during the Johnston Atoll accident (Wolf et al., 1997).

The U-Lα and Pu-Lα ratios obtained from SEM–EDX spot measurements of particle surfaces indicated local variation within a particle, variations between particles from the same site (Figs. 2B and 3 B) as well as between Thule and Palomares particles.

To provide semi-quantitative information of the actinide distribution on the particle surfaces, Pu-Lα and U-Lα X-ray intensities were obtained from ESEM–EDX line scans (Figs. 4 and 5). The Pu-Lα/U-Lα ratio on the surfaces of Palomares particles ($n=3$ particles) varied from 0.5 to 2.0, with a mean ratio of 1.0 for all three line scanned particles (Fig. 4, Table 2). The corresponding ratio varied between 0.2–0.6 for individual Thule particles, while the mean ratios of TA and TB were found to be 0.5 and 0.3, respectively (Fig. 5, Table 2). Taking the uncertainties into account, the investigated Palomares particles feature higher mean Pu-Lα/U-Lα ratios of line scans than for the Thule particles. Based on the line scans the variations in the Pu/U distribution were more pronounced for Palomares than for Thule particles.

Based on line scans across individual particles, local Pu-Lα/U-Lα ratios deviating from the mean ratio indicated heterogeneities on a 1–2 μm scale or less (Figs. 4D, 5B). Some of the observed Pu-Lα/U-Lα ratio variations may be attributed to physical effects including topographic effects that influence the interactions of electrons and the propagation of X-rays. However, "hot spot" areas (inclusions) observed as bright white areas in BEI images were clearly associated with low Pu-Lα/U-Lα ratios well below 2 standard deviations of the mean of the scanned lines. Thus, the inclusions are enriched with respect to U and depleted in Pu compared to the surrounding material. Such surface heterogeneities were observed for particles from both sites, and are attributed to the microstructure of the original fissile material or processes involving fragmentation of the weapons and formation of particles (i.e. release conditions), although preferential leaching of actinides cannot be excluded. Using SEM and ATEM, inclusions of actinides with widely varying Pu/U ratios have also been observed in discrete radioactive particles isolated from Johnston Atoll soil samples (Wolf et al., 1997).

3.3. μ-XANES

XANES are used to provide information on the oxidation state of actinides (Salbu et al., 2003; Powell et al., 2006). By tuning the energy of an X-ray beam (with a monochromator) over the ionization energy of a shell, an abrupt increase in the absorption occurs, termed the absorption edge. The features of absorption edges and peaks (white lines) are influenced by the chemical speciation of the absorbing element, i.e. the energy and shape of the spectra are correlated with valence and site symmetry (Conradson et al., 1998). Decreased shielding of core electrons with increasing valence results in increased binding energy of core electrons and can be observed as a chemical shift in the XANES spectra. The most important factors determining the XANES spectra of U and Pu oxides are the valence state and the presence or absence of actinyl species. To differentiate between oxidation states appropriate well-defined oxidation state

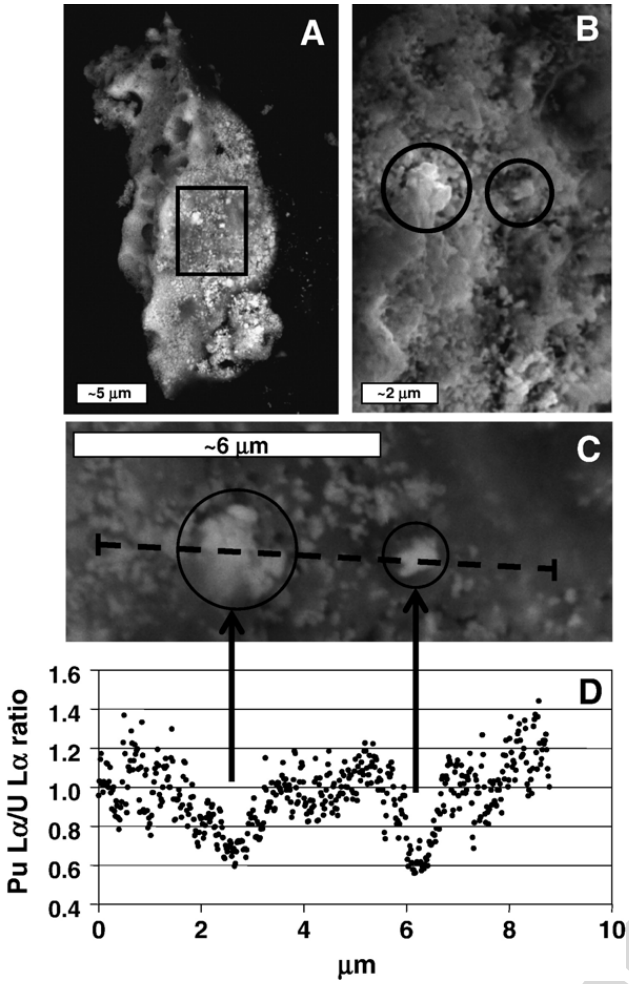

Fig. 4. ESEM line scan analysis of a Palomares particle (PA). (A) BEI image of the whole particle shows bright areas indicating high average atomic number area heterogeneities. (B) SEI image of the bright area highlighted in (A) at higher magnification, shows the agglomerated structure of the spots. (C) BEI image of the analysed area including the two bright spots in (B). The location of the scanned line is indicated. (D) Pu-Lα/U Lα intensity ratios along a ~9 µm line scanned over the area in (B and C). Resolution ~1 µm.

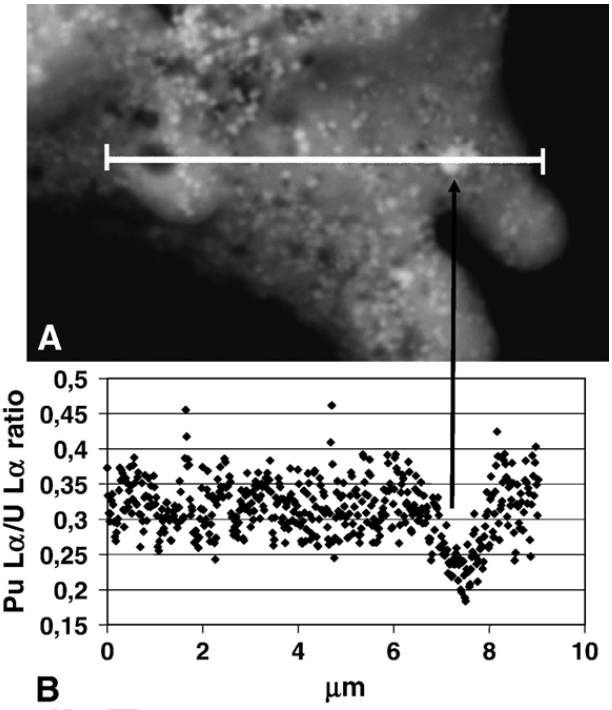

Fig. 5. ESEM line scan analysis of Thule particle TB. (A) BEI image of the analysed area including a bright spot indicating a high average atomic number area. The location of the scanned line is indicated. (B) Pu-Lα/U Lα intensity ratios along a ~9 µm line scanned over the area indicated in (A). Resolution ~1 µm.

standards should be applied. As no well-defined mixed Pu/U-oxide standards are available or published in literature, the XANES profiles of the Palomares and Thule particles are compared with well-defined U oxide standards and a variety of Pu-XANES profiles from the literature.

Based on the shape, position of the WL and the FSM of the U- and Pu-L_{III} fluorescent XANES profiles (uncorrected for self-absorption), the oxidation states for U and Pu in Palomares and Thule particles were remarkably similar, in view of the different environmental conditions they have been exposed to (Figs. 6 and 7). No differences in oxidation states were apparent between the cores and the outer spheres of the investigated particles using the 20 µm lateral resolution setup. Apparently all U and Pu in the investigated Palomares and Thule particles were oxidised and the matrix of the particles could be characterized as a mixture of U and Pu oxides.

Based on the shape, position of the WL and the FSM, the U L_{III} XANES profiles of particles PB, TA and TB in Fig. 6 essentially overlap with the UO_2 standard profile, indicating that the U was present as U(IV). Especially for Palomares particle PC, the WL and inflection point were shifted towards higher energy and was found midway between those of the UO_2 and U_3O_8 standards, indicating a mixture of UO_2 and U_3O_8. No U metal or U(VI) in the form of uranyl could be observed. If the original material contained metallic U, oxidation to UO_2 and U_3O_8 could easily occur during the explosive fire, as observed for impacted depleted uranium ammunitions (Salbu et al., 2003, 2004). If the original weapon material was made

Table 2
Pu-Lα/U-Lα intensity ratios of the investigated particles obtained by ESEM–EDX line scan

Method	Information	Palomares	*n*	Thule	*n*
EDX line scan, mean	Particle surface	1.0	3	0.3, 0.5	2
EDX line scan, range	Particle surface	0.5–2.0	3	0.2–0.6	2
EDX line scan, BEI features	Surface inclusion	0.5–0.6	3	0.2	1

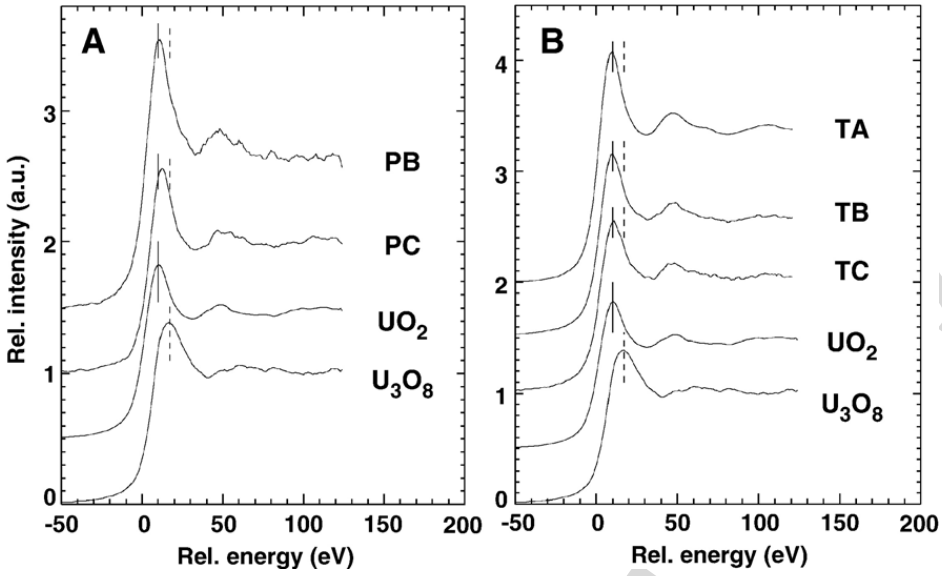

Fig. 6. Fluorescent U L_{III} μ-XANES profiles obtained from (A) Palomares (this work) and (B) Thule particles (Lind et al., 2005) in comparison to UO_2 and U_3O_8 reference compounds.

from UO_2, only a moderate oxidation takes place during the explosive fire. At high temperature and pressure conditions in the presence of air a mixture of UO_2 and U_3O_8 (and possibly other intermediate forms) can be expected, as observed for UO_2 particles released during the Chernobyl fire (Salbu et al., 2001). The presence of U_3O_8 would increase the particle weathering rates.

Based on the shape, energy position of the WL and the FSM and a comparison with recently published Pu-L_{III} XANES profiles of solid compounds and standard solutions, Pu in all the particles investigated was apparently present as Pu(III)/Pu(IV), Pu(IV)/Pu(V) or a mixture of these oxidation states, whereas energy shifts or features corresponding to Pu(VI) and metallic Pu could not be identified. This interpretation is based on three observations.

Firstly, a significant contribution of Pu metal to the particle composition seems unlikely as the negative energy shifts compared to Pu(IV) were small and no indications of a substantially diminished WL were observed for any of the XANES profiles. Secondly, in contrast to recent reports on Thule particles (Eriksson et al., 2005) and Johnston

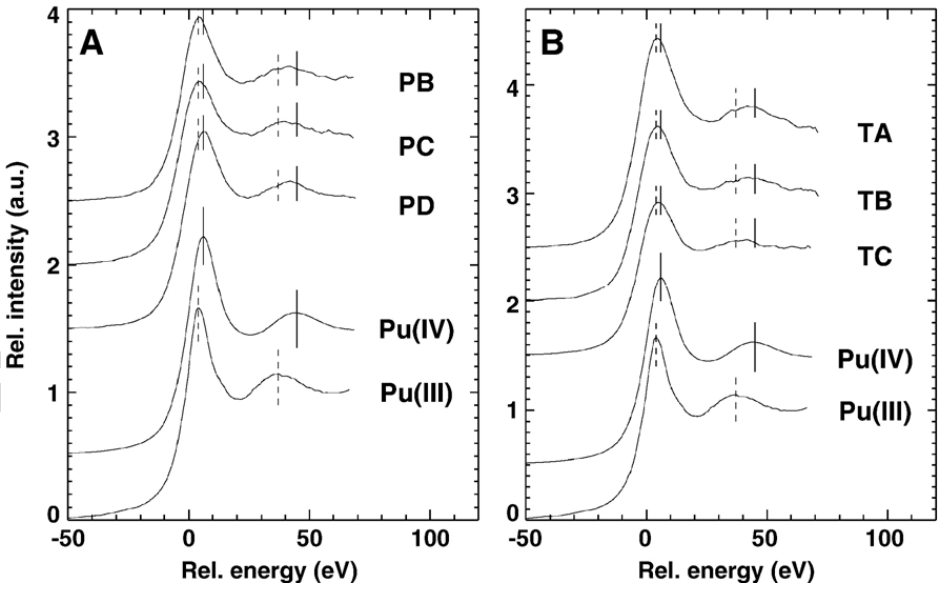

Fig. 7. Flourescent Pu-L_{III} μ-XANES profiles obtained from Palomares (this work) and Thule (Lind et al., 2005) particles in comparison to Pu(III) and Pu(IV) reference profiles.

Atoll particles (Wolf et al., 1997) there were no indication of the presence of appreciable amounts of Pu(VI). No shift (of WL or inflection points) towards higher energies compared to the Pu(IV) reference profile was observed in the Palomares and Thule particles. Finally, the WL energies of the particles fall within the range of $PuO_{2+x-y}(OH)_{2y}$ zH_2O materials (18,068.2–18,069.8 eV) in which x can vary from −0.5–0.25 and Pu is predominately present as Pu(IV) with varying amounts of Pu(V) contributing to the x (Conradson et al., 2004a; 2005). The energy difference between the WL centroid and FSM in the particles vary within 35–38 eV, i.e. somewhere midway between Pu(III) and Pu(IV). A mixture of Pu(IV)/Pu(V) should give XANES energies at or slightly below that of PuO_2 (Conradson et al., 2005), and somewhat similar to what would be expected for a mixture of Pu(III) and Pu(IV). Thus, the differentiation between Pu (III), (IV) and (V) in oxides is difficult to attain from XANES only. According to (Conradson et al., 2004b) $PuO_{2+x-y}(OH)_{2y}$ zH_2O is formed upon oxidation of Pu, while ordered PuO_2 is quite rare and is only attained under low H_2O and relatively low O_2 conditions. Thus, the presence of ordered PuO_2 can probably be disregarded under environmental conditions such as in Palomares soils and Thule sediments. Based on these interpretations, no appreciable amounts of Pu(0) and Pu(VI) are present in the investigated particles, whereas the presence of Pu(III)/Pu (IV), Pu(IV)/Pu(V) or a mixture of all three oxidation states should be taken into account.

Dispersion of particulate oxidised Pu is expected to occur if Pu metal or Pu oxide is involved in a fire or explosion such as those at Palomares and Thule (Martz and Haschke, 1998). The oxidation of Pu metal may have been partial, thus providing a tentative route of formation for particles with a mixture of Pu(III) and Pu(IV) and even higher oxidation states. If the original material was made of PuO_2 the formation of PuO_{2+x} ($x>0$) in the presence of moisture seems likely to have occurred (Haschke and Oversby, 2002) during the explosive fire or due to subsequent environmental weathering since 1966. The oxidation would, however, probably not exceed the $PuO_{2.25}$ hyperstoichiometric end point (Conradson et al., 2004b). It has been reported that substoichiometric oxides more readily soluble than PuO_2, e.g. Pu_2O_3, may form at temperatures above 1400 °C due to loss of oxygen from Pu oxide (Keller, 1971; Sill, 1975). Temperatures in fuel fires are known to approach 1000 °C and are expected in propellant fires to exceed 2000 °C (Haschke and Martz, 1998). Thus, the temperature regime required to expel oxygen from Pu oxide cannot be ruled out and hence the possible presence of Pu(III) in Palomares and Thule particles should not be excluded.

Taking all XANES results into account, it appears that the Palomares and Thule particles contain a mixture of U (predominately IV with the presence of VI) and Pu ((III)/(IV), (IV)/(V) or (III), (IV) and (V)), most probably in the form of mixed-oxides/oxyhydroxides and not as ordered actinide-O_2 structures. The fact that U and Pu coexist in the particles as mixed oxides has implications for predicting both the overall particle weathering rates as well as their remobilisation potential. Previous studies of U and Pu mixed-oxide materials suggest that U mixed with Pu in particle matrices may lead to a higher dissolution of Pu than for pure Pu oxide materials (Eidson and Mewhinney, 1983). Thus, the prediction of solubility properties of Pu/U mixed oxide particles can hardly be derived from binary oxide studies, i.e. oxides of U and Pu studied separately. Furthermore, the presence of U oxidation states higher than+IV and trivalent and/or pentavalent Pu may also imply that partial leaching may take place over time, as observed for Palomares during the last 20 years.

4. Conclusions

The present work demonstrates that particles originating from the Palomares and Thule accidents contain a mixture of enriched U and weapon-grade Pu material. The $^{239}Pu/^{235}U$ ratio is a factor of 1.3 higher for the measured Palomares particle than for the particle from Thule. SEM–EDX mapping and SR-based μ-XRF mapping indicated that U and Pu were homogeneously distributed in the particles. However, results from ESEM–EDX line scan analyses with ~1 μm resolution revealed that U and Pu are co-localised on all investigated particle surfaces, but that surface inclusions enriched with respect to U and depleted with respect to Pu compared to the surrounding material were observed for particles from both sites. The microstructures of the particles are attributed to the original fissile material or processes involving fragmentation of the weapons and formation of particles, although weathering and subsequent releases of actinides from the particle surfaces cannot be excluded.

Based on μ-XANES, the particle matrices are U and Pu oxide mixtures, most probably in the form of mixed oxides/oxyhydroxides. The oxidation state of U seems to be predominately+IV (UO_2) with a minor and variable contribution of higher oxidation states (U_3O_8), while Pu seems to be present as Pu(III)/Pu(IV), Pu(IV)/Pu(V) or a mixture of all three oxidation states. Neither metallic U or Pu nor uranyl or Pu(VI) could be observed.

As Pu in Pu/U mixtures might be more soluble than PuO_2, as the oxidation states for Pu/U oxides may differ from+4 and as Pu/U heterogeneities are observed on particle surfaces the results indicate that the particles

represent a higher remobilisation potential than previously anticipated, as also observed during the last decades in Palomares.

Despite the low number of particles analysed, the present work reveals that the Palomares and Thule particles as phenomena are remarkably similar with respect to elemental distributions, morphology and oxidation states reflecting that they originate from similar source and release scenarios. Furthermore, particle characteristics are more dependent on factors determined by the source and the release scenario than the environmental conditions. Particle weathering and subsequent mobilisation of U and Pu will depend on particle characteristics, while the behaviour of Pu released from the particles will be dependent on the surrounding environment.

The present work has demonstrated that a combination of advanced analytical techniques can provide unique information on the solid-state speciation of nuclear fissile material released into the environment. For areas contaminated with radioactive particles, information on particle characteristics influencing weathering rates should be included in the impact assessments, and the techniques described in the present work should be considered as useful tools.

Acknowledgements

We gratefully acknowledge the support provided by the European Commission (contracts no. IHP-Contract HPRI-CT-1999–00040/2001–00140 and FIGE-CT-2000–00108), IAEA (CRP, "Radiochemical, Chemical and Physical Characterization of Radioactive Particles in the Environment") and the Norwegian Research Council (project no. 141479/720). The authors are indebted to Gerald Falkenberg (HASYLAB BL) for beamline assistance with the μ-XANES measurements, Melissa A. Denecke (Forschungszentrum Karlsruhe) for graciously making the Pu-XANES reference profiles available to us and for her constructive comments, Rajdeep Singh Sidhu for valuable comments and to Lindis Skipperud and Trygve Krekling (UMB) for ICP-MS and SEM/ESEM assistance, respectively.

References

Aarkrog A. Radioecological investigation of plutonium in an arctic marine environment. Health Phys 1971;20:31–47.

Bukharin OA. Securing Russia's HEU stocks. Sci Glob Secur 1998;7:311–31.

Chamizo E, Garcia-Leon M, Synal HA, Suter M, Wacker L. Determination of the $^{240}Pu/^{239}Pu$ atomic ratio in soils from Palomares (Spain) by low-energy accelerator mass spectrometry. Nucl Instr and Meth A 2006;249:768–71.

Choppin GR. Actinide speciation in the environment. Radiochim Acta 2003;91:645–9.

Clacher A. Development and Application of Analytical Methods for Environmental Radioactivity. University of Manchester; 1995.

Conradson SD, Al Mahamid I, Clark DL, Hess NJ, Hudson EA, Neu MP, et al. Oxidation state determination of plutonium aquo ions using X-ray absorption spectroscopy. Polyhedron 1998;17:599–602.

Conradson SD, Abney KD, Begg BD, Brady ED, Clark DL, Den Auwer C, et al. Higher order speciation effects on plutonium L-3 X-ray absorption near edge spectra. Inorg Chem 2004a;43:116–31.

Conradson SD, Begg BD, Clark DL, Den Auwer C, Ding M, Dorhout PK, et al. Local and nanoscale structure and speciation in the $PuO_{2+x-y}(OH)_{2y}zH_2O$ system. J Am Chem Soc 2004b;126:13443–58.

Conradson SD, Begg BD, Clark DL, Den Auwer C, Ding M, Dorhout PK, et al. Charge distribution and local structure and speciation in the UO_{2+x} and PuO_{2+x} binary oxides for $x \leq 0.25$. J Solid State Chem 2005;178:521–35.

Dahlgaard H, Eriksson M, Ilus E, Ryan T, McMahon CA, Nielsen SP. Plutonium in the marine environment at Thule, NW-Greenland after a nuclear weapons accident. In: Kudo A, editor. Plutonium in the environment. Oxford: Elsevier; 2001. p. 15–30.

Dahlgaard H, Eriksson M, Nielsen SP, Joensen HP. Levels and trends of radioactive contaminants in the Greenland environment. Sci Total Environ 2004;331:53–67.

Denecke MA. Actinide speciation using X-ray absorption fine structure spectroscopy. Coord Chem Rev 2006;250:730–54.

Drell S, Peurifoy B. Technical issues of a nuclear test ban. Annu Rev Nucl Part Sci 1994;44:285–327.

Duff MC, Hunter DB, Triay IR, Bertsch PM, Reed DT, Sutton S, et al. Mineral associations and average oxidation states of sorbed Pu on tuff. Environ Sci Technol 1999;33:2163–9.

Eidson AF, Mewhinney JA. *In vitro* dissolution of respirable aerosols of industrial mixed uranium and plutonium mixed-oxide nuclear fuels. Health Phys 1983;45:1023–37.

Eriksson Mats. On Weapons Plutonium in the Arctic Environment (Thule, Greenland). Risø National Laboratory; 2002. p. 1–146. 3–5–0002.

Eriksson M, Osan J, Jernstrom J, Wegrzynek D, Simon R, Chinea-Cano E, et al. Source term identification of environmental radioactive Pu/U particles by their characterization with non-destructive spectrochemical analytical techniques. Spectrochim Acta B 2005;60:455–69.

Espinosa A, Aragon A, de la Cruz B, Gutiérrez J. Influence of cow urine in the bioavailability of plutonium oxide particles in Palomares soils. Radioprotection 2005;40:S73–7.

Felmy AR, Rai D, Schramke JA, Ryan JL. The solubility of plutonium hydroxide in dilute-solution and in high-ionic-strength chloride brines. Radiochim Acta 1989;48:29–35.

García-Tenorio R, Manjón G, Jiménez-Ramos MC, Vioque IA, García-León M. In: Mitchell P, Vintro LL, editors. EU ADVANCE FINAL REPORT. Dublin: University College Dublin; 2004.

Haschke JM, Martz JC. Oxidation kinetics of plutonium in air from 500 to 3500 °C — application to source terms for dispersal. J Alloys Compd 1998;266:81–9.

Haschke JM, Oversby VM. Plutonium chemistry: a synthesis of experimental data and a quantitative model for plutonium oxide solubility. J Nucl Mater 2002;305:187–201.

Iranzo E, Salvador S, Iranzo CE. Air concentrations of 239Pu and 240Pu and potential radiation doses to persons lining near Pu-contaminated areas in Palomares, Spain. Health Phys 1987;52:453–61.

Irlweck K, Hrnecek E. Am-241 concentration and Pu-241/Pu-239 (240) ratios in soils contaminated by weapons-grade plutonium. J Radioanal Nucl Chem 1999;242:595–9.

Jiménez-Ramos MC, García-Tenorio R, Vioque I, Manjon G, García-Leon M. Presence of plutonium contamination in soils from Palomares (Spain). Environ Pollut 2006;142:487–92.

Jiménez-Ramos MC, Barros H, Garcia-Tenorio R, Garcia-Leon M, Vioque I, Manjon G. On the presence of enriched uranium in hot-particles from the terrestrial area affected by the Palomares accident (Spain). Environ Pollut 2007;145:391–4.

Kashparov VA, Oughton DH, Protsak VP, Zvarisch SI, Levchuk SE. Kinetics of fuel particle weathering and ^{90}Sr mobility in the Chernobyl 30 km exclusion zone. Health Phys 1999;76:251–9.

Keller C. The Chemistry of the Transuranium Elements. Weinheim: Verlag Chemie GmbH; 1971. 380–381 pp.

Kim JI, Kanellakopulos B. Solubility products of plutonium(IV) oxide and hydroxide. Radiochim Acta 1989;48:145–50.

Knopp R, Neck V, Kim JI. Solubility, hydrolysis and colloid formation of plutonium(IV). Radiochim Acta 1999;86:101–8.

Lind OC, Salbu B, Janssens K, Proost K. In: Mitchell P, Vintro LL, editors. EU ADVANCE FINAL REPORT. Dublin: University College Dublin; 2004.

Lind OC, Salbu B, Janssens K, Proost K, Dahlgaard H. Characterization of uranium and plutonium containing particles originating from the nuclear weapons accident in Thule, Greenland, 1968. J Environ Radioact 2005;81:21–32.

Martz JC, Haschke JM. A mechanism for combustive heating and explosive dispersal of plutonium. J Alloys Compd 1998;266: 90–103.

Mitchell PI, Leon Vintro L, Dahlgaard H, Gasco C, Sanchez-Cabeza JA. Perturbation in the Pu-240/Pu-239 global fallout ratio in local sediments following the nuclear accidents at Thule (Greenland) and Palomares (Spain). Sci Total Environ 1997;202:147–53.

Panak PJ, Booth CH, Caulder DL, Bucher JJ, Shuh DK, Nitsche H. X-ray absorption fine structure spectroscopy of plutonium complexes with Bacillus sphaericus. Radiochim Acta 2002;90:315–21.

Powell BA, Duff MC, Kaplan DI, Fjeld RA, Newwille M, Hunter DB, et al. Plutonium oxidation and subsequent reduction by Mn (IV) minerals in Yucca mountain tuff. Environ Sci Technol 2006;40:3508–14.

Runde W, Conradson SD, Efurd DW, Lu NP, VanPelt CE, Tait CD. Solubility and sorption of redox-sensitive radionuclides (Np, Pu) in J-13 water from the Yucca mountain site: comparison between experiment and theory. Appl Geochem 2002;17:837–53.

Salbu B. Source-related characteristics of radioactive particles: a review. Radiat Prot Dosim 2000a;92:49–54.

Salbu B. Speciation of Radionuclides in the Environment. In: Meyers RA, editor. Encyclopedia of Analytical Chemistry. Chichester: John Wiley & Sons Ltd; 2000b. p. 12993–3016.

Salbu B, Krekling T, Lind OC, Oughton DH, Drakopoulos M, Simionovici A, et al. High energy X-ray microscopy for characterisation of fuel particles. Nucl Instr Methods A 2001;467: 1249–52.

Salbu B, Janssens K, Lind OC, Proost K, Danesi PR. Oxidation states of uranium in DU particles from Kosovo. J Environ Radioact 2003;64:167–73.

Salbu B, Janssens K, Lind OC, Proost K, Gijsels L, Danesi PR. Oxidation states of uranium in depleted uranium particles from Kuwait. J Environ Radioact 2004;78:125–35.

Sill CW. Some problems in measuring plutonium in environment. Health Phys 1975;29:619–26.

Silva RJ, Nitsche H. Environmental actinide science. MRS Bull 2001;26:707–13.

Wolf SF, Bates JK, Buck EC, Dietz NL, Portner JA, Brown NR. Physical and chemical characterization of actinides in soil from Johnston Atoll. Environ Sci Technol 1997;31:467–71.

Zaitseva VP, Alekseeva DP, Gel'man AD. Hydrolysis of nitric acid solutions of plutonium(V). Sov Radiochem 1968;10:526–9.